Photochemistry and Photobiology, 2004, 80: 000–000

Invited Review

Quantum Dot Nanocrystals for *In Vivo* Molecular and Cellular Imaging¶

Andrew M. Smith, Xiaohu Gao and Shuming Nie*

Departments of Biomedical Engineering and Chemistry, Emory University and Georgia Institute of Technology, Atlanta, GA

Received XX/XX/XX; accepted 15 July 2004

ABSTRACT

Semiconductor quantum dots (QD) are nanometer-sized crystals with unique photochemical and photophysical properties that are not available from either isolated molecules or bulk solids. In comparison with organic dyes and fluorescent proteins, QD are emerging as a new class of fluorescent labels with improved brightness, resistance against photobleaching and multicolor fluorescence emission. These properties could improve the sensitivity of biological detection and imaging by at least 10- to 100-fold. Further development in high-quality near-infrared–emitting QD should allow ultrasensitive and multicolor imaging of molecular targets in deep tissue and living animals. Here, we discuss recent developments in QD synthesis and bioconjugation, applications in molecular and cellular imaging as well as promising directions for future research.

INTRODUCTION

Quantum dots (QD) are nanometer-sized semiconductors with size-tunable optical and electronic properties. Recent research has shown that QD can be covalently linked with biorecognition molecules such as peptides, antibodies, nucleic acids, and small molecules for use as fluorescent probes (1–4). The results demonstrate that bioconjugated QD probes are similar in size to fluorescent proteins and do not suffer from major kinetic or steric hindrance problems (5–7). In addition, QD-encoded beads have been developed by incorporating multicolor QD into polymer beads at precisely controlled ratios (8). With each embedded with a spectroscopic signature or ''bar code,'' these encoded beads are being developed for applications in multiplexed bioassays, medical diagnostics and combinatorial synthesis. Indeed, QD have enjoyed considerable academic and commercial success because of their broad applications in biology and medicine.

QD research started with the realization that the optical and electronic properties of small semiconductor particles were strongly dependent on particle size due to quantum confinement of the charge carriers in small spaces. A theoretical framework for these size-dependent properties was described by Al. L. Efros and A. L. Efros (9) and Ekimov and Onushchenko (10) in 1982. During the next 2 decades, extensive research was carried out for potential applications in optoelectronic devices, quantum dot lasers and high-density memory. In 1998 two groups, one led by Alivisatos at UC-Berkeley and another led by Nie (then at Indiana University–Bloomington), simultaneously demonstrated that semiconductor QD could be made water soluble and could be conjugated with biological molecules (2,4). However, their biological applications were still limited by problems with surface chemistry and by the lack of widely (commercially) available materials. In the past 2 years QD have finally come of age, thanks to major improvements in surface modification and bioconjugation (11).

QUANTUM CONFINEMENT AND SIZE-TUNABLE PROPERTIES

QD are somewhat spherical nanocrystals in the size range of 1–10 nm diameter (12,13). Semiconductor nanocrystals can also be produced with other shapes such as rods and tetrapods (14), but spherical QD are the most widely used for biological applications and, therefore, will be the focus of this article. One of the most intriguing features of QD is that the particle size determines many of the QD properties, most importantly the wavelength of fluorescence emission. By altering the QD size and its chemical composition, fluorescence emission may be tuned from the near ultraviolet, throughout the visible and into the near-infrared (NIR) spectrum, spanning a broad wavelength range of 400–2000 nm (15–19). To understand these properties, we briefly discuss the photophysics of bulk phase semiconductors in the next section.

Bulk semiconductor physics

Solid state physics often divides materials into three categories based on electrical conductivity: conductors, semiconductors and insulators (see Fig. 1A). The conductivity of a solid is frequently rationalized as the difference in energy between the valence and conduction bands of the material. In solid state materials, discrete electronic orbitals from individual atoms combine to form wide,

¶Posted on the website on

*To whom correspondence should be addressed: Departments of Biomedical Engineering and Chemistry, Emory University and Georgia Institute of Technology, 1639 Pierce Drive Suite 2001, Atlanta, GA 30332, USA. Fax: 404-727-9873; e-mail: snie@emory.edu

Abbreviations: CdSe, cadmium selenide; EGF, epidermal growth factor; EPR, enhanced permeability and retention; FRET, fluorescence resonance energy transfer; MRI, magnetic resonance imaging; NIR, near-infrared; PEG, polyethylene glycol; QD, quantum dots; RES, reticuloendothelial system; TOPO, trioctylphosphine oxide.

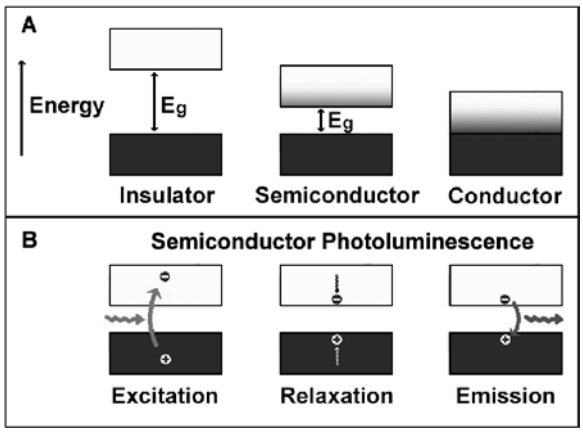

Figure 1. Schematic diagrams showing bandgaps and charge carriers in bulk materials. A: Solid state materials are classified as either electrical insulators, semiconductors or conductors, depending on the bandgap energy (E_g) between the valence and conduction bands. The valence bands are below the conduction bands for each material type, and electron occupation is represented by blue shading. At room temperature, electrons partially occupy the conduction bands in semiconductors and conductors, but the bandgap energy is too large for thermal electronic excitation in insulators. B: Semiconductor photoluminescence is illustrated in three separate steps. Absorption of a photon causes the excitation of an electron, generating charge carriers, an electron in the conduction band and a hole in the valence band. These two carriers quickly lose energy as they relax to the band edges, and their recombination leads to the emission of a photon. The energy relaxation process causes a Stokes shift, toward longer wavelengths relative to the excitation light wavelength. This process is valid only for direct bandgap semiconductors because indirect bandgap semiconductors require phonon assistance for momentum conservation for each electronic transition.

nearly continuous bands of electronic energy states. The valence band is the highest electronic energy level that is occupied with electrons at room temperature. Likewise, the conduction band is the lowest energy electronic state that is not occupied by electrons, although thermal excitation may allow it to be partially occupied. An electron in the valence band may gain energy (thermally or by the absorption of a photon) to enter the conduction band, thus leaving behind a positively charged hole in the valence band. Electron–hole pairs are charge carriers and may be mobilized in opposite directions by an applied voltage bias. The difference in energy between the valence and conduction bands, called the bandgap energy (E_g, typically expressed in electron volts [eV]), determines the energy that must be gained for an electron to enter the conduction band. Thus, insulators are characterized by a wide bandgap, such that electrons do not have enough thermal energy at room temperature to overcome the energy barrier to occupy the conduction band, thus making conductivity extremely low. The bandgaps of semiconductors are small enough that some electrons may be thermally excited at room temperature to form charge carriers. The conduction and valence bands overlap in conductors, forming a continuous band, so that there is little resistance to current flow with an applied voltage.

To generate mobile charge carriers in a semiconducting material, electrons must gain energy greater than or equal to the bandgap energy. Once in the excited state, a conduction-band electron may relax back to its ground state in the valence band through radiative recombination with a hole, resulting in the emission of a photon with the same energy as the bandgap (see Fig. 1B). Light emission is only one of the many possible decay processes, but it is of both fundamental and practical importance. Because the bandgap dictates the fluorescence emission wavelength, considerable effort has been devoted to engineer semiconductor materials and alloys with precisely tuned bandgaps for use in lasers, photodiodes and other optoelectronic devices.

QD photophysics

A fascinating property of semiconductors is that the bandgap is not only dependent on composition but also on the particle size. Typically referred to as the ''quantum confinement effect,'' this size dependence is readily observed when one or more dimensions of a semiconductor are reduced to the nanometer regime. Confinement of one dimension can be accomplished through the fabrication of thin sheets of semiconductors called quantum wells. Two-dimensional confinement leads to quantum wires that conduct electricity along only one axis. If all three dimensions are confined to the nanometer scale, the semiconductor is called a QD, which has properties in between bulk phase crystals and individual isolated atoms.

The change in bandgap energy with crystal size is most accurately described by using quantum mechanical models, but a qualitative ''particle in a box'' analogy is useful to understand the main principles (20–22). An important concept of quantum mechanics is that matter may behave like a wave, such that single particles, like electrons and holes, may be described mathematically using wave functions. An electron that is free to move infinitely in all directions would have a wave function defined at all points in space, and the electron would theoretically occupy all points simultaneously. Restricting its position between barriers of infinite height would cause the electron to have a zero probability of occupying positions outside of this ''box.'' A result of this restriction is that the ground state kinetic energy of the particle must increase to satisfy the Heisenberg uncertainty principle. This rule states that if the position of a particle is well defined (such as in a box), then the momentum cannot be zero, thus giving the particle nonzero kinetic energy. As the size of the box decreases, the ground state energy must increase to accommodate this additional restriction in position. A QD is like a spherical box containing two particles, an electron and a hole. Much like a particle in a box, the kinetic energies of these two carriers increase as the size of the QD decreases, so more energy is required to create these particles, and more energy is released when these two particles annihilate one another through recombination. As a result, both the excitation and emission spectra shift to shorter wavelengths (higher energies) with decreasing particle size. The quantitative descriptions for the quantum confinement effect are more complex because of the noninfinite nature of the potential well and other factors such as reduced carrier masses and electrostatic attractions between the electron and hole (22–24).

This dependence of light emission on particle size allows the development of new fluorescence emitters with precisely tuned emission wavelengths. For example, the semiconductor cadmium selenide (CdSe) has a bulk bandgap of 1.7 eV (corresponding to 730 nm light emission). QD of this material can be tuned to emit between 450–650 nm by changing the nanocrystal diameter from 2 to 7 nm (Fig. 2A). The composition of the material may also be used as a parameter to alter the bandgap of a semiconductor. QD with a diameter of 5 nm can be tuned to emit between 610–800 nm by changing the composition of the alloy $CdSe_xTe_{1-x}$ (Fig. 2B).

Comparison with organic dyes

Organic fluorophores are widely used as biological labels for fluorescence imaging and detection. Because the spectroscopic

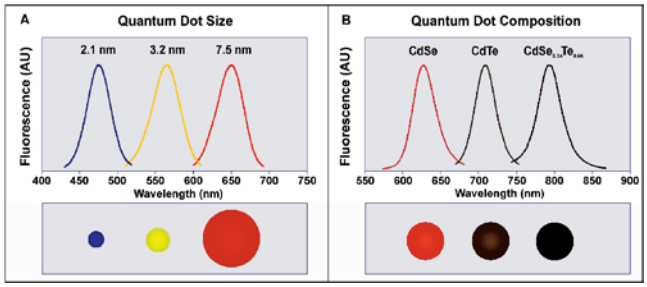

Figure 2. Size and composition tuning of optical emission for binary CdSe and ternary CdSeTe quantum dots. A: CdSe QD with various sizes (given as diameter) may be tuned to emit throughout the visible region by changing the nanoparticle size while keeping the composition constant. B: The size of QD may also be held constant, and the composition may be used to alter the emission wavelength. In the above example, 5 nm diameter quantum dots of the ternary alloy $CdSe_xTe_{1-x}$ may be tuned to emit at longer wavelengths than either of the binary compounds CdSe and CdTe because of a nonlinear relationship between the alloy bandgap energy and composition (17).

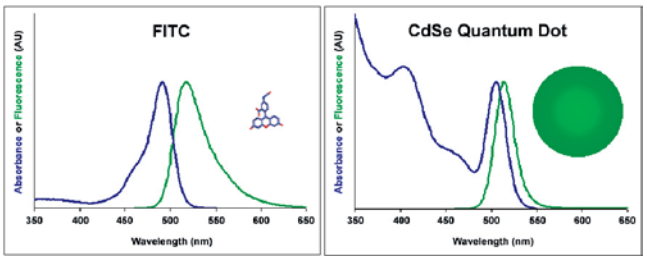

Figure 3. Comparison of absorbance (blue) and fluorescence (green) spectra between organic dyes (fluorescein isothiocyanate [FITC]) and CdSe quantum dots with the same emission wavelength. Note that the emission peak is more narrow and symmetric for the QD spectrum, and the absorption band extends far into the ultraviolet region. The size differences of FITC and QD are also shown.

properties of QD are fundamentally different from that of organic dyes, QD could open new possibilities in a number of research areas. As shown in Fig. 3, QD have broad excitation profiles and narrow/symmetric emission peaks (commonly 25–35 nm full width at half maximum) (25). Therefore, multicolored QD could be simultaneously excited with a single light source, with minimal spectral overlap, providing significant advantages for multiplexed detection of molecular targets. Furthermore, QD have been shown to remain brightly emissive after long periods of excitation, whereas organic dyes are photobleached quickly (2,4,5). For these reasons, QD provide the possibility of continuous, real-time imaging of single molecules and single cells over an extended period of time.

QD can be tuned to emit in a range of wavelengths by changing the nanoparticle size and composition, whereas new organic dyes must be developed to shift their emission wavelengths. This tunability allows the synthesis of QD that emit in the NIR spectrum, which is optimal for deep fluorescence imaging in living organisms (26,27). Most organic dyes with NIR emission suffer from low quantum yields, rapid photobleaching, poor stability/aggregation or a combination of these problems (28,29). It is worth noting, however, that QD may not be suitable for applications in which the probe size must be minimized, such as intermolecular interaction studies where steric hindrance could interfere with biomolecular function. Dyes are typically an order of magnitude smaller than QD and will continue to be useful in these studies (Fig. 3). Organic fluorophores have other properties (*e.g.* self-quenching) that could be problems in some cases but could be valuable for other applications such as activatable molecular beacon probes (see Future Directions for further discussion on QD biosensors and activatable probes).

SYNTHESIS AND BIOCONJUGATION

Synthesis and capping

The prototypical QD is CdSe because colloidal syntheses for monodispersed nanocrystals of this semiconductor are well established. CdSe is most often synthesized through the combination of cadmium and selenium precursors in the presence of a QD-binding ligand that stabilizes the growing QD particles and prevents their aggregation into bulk semiconductors. Among various synthetic methods reported in the literature, high-temperature synthesis in coordinating solvents has yielded the best-size monodispersity and fluorescence efficiencies. A coordinating solvent serves as a solvent and as a ligand and is most commonly a mixture of trioctylphosphine, trioctylphosphine oxide (TOPO) and hexadecylamine (15,30). The basic functional groups of these ligands (phosphines, phosphine oxides and amines) attach to the QD surface during synthesis, leaving the ligand alkyl chains directed away from the surface. The resulting QD are highly hydrophobic and only soluble in nonpolar solvents such as chloroform and hexane.

The CdSe core is often capped with a thin layer of a higher bandgap material such as ZnS or CdS. This ''shell'' removes surface defects and prevents nonradiative decay, leading to a significant improvement in fluorescence quantum yields (from 5% to more than 50%) (31). As mentioned above, many different processes are available for an electron to relax to its ground state after excitation. These include nonradiative recombination events that decrease the efficiency of optoelectronic devices and decrease the fluorescence efficiency of QD. For QD, the surface atoms constitute a large percentage of the total atoms of the crystal due to the high surface area-to-volume ratio of small colloidal particles. Therefore, surface-related recombination due to localized trapping of carriers is thought to be one of the main factors that reduce the emission efficiencies of QD (32). These surface-related recombinations may be minimized by confining the electron and hole to the core of the crystal through surface passivation. The use of a higher bandgap semiconductor confines the charge carriers to the core QD, thus minimizing surface recombination. CdSe is normally passivated with zinc sulfide, resulting in a structure referred to as (CdSe)ZnS or CdSe/ZnS, but zinc selenide and cadmium sulfide are also commonly used (31,33,34).

Water solubilization

For use in biological labeling, QD must be rendered hydrophilic so that they are soluble in aqueous buffers. Two general strategies have been developed for phase transfer of QD to aqueous solution (Fig. 4). In the first approach, hydrophobic surface ligands are replaced with bifunctional ligands such as mercaptoacetic acid, which contains a thiol group that binds strongly to the QD surface as well as a carboxylic acid group that is hydrophilic (2). Other functional groups may also be used; for example, silane groups can be polymerized into a silane shell around the QD after ligand exchange (4). In the second method, coordinating ligands (*e.g.* TOPO) on the QD surface are used to interact with an amphiphilic polymer (5,35) such as octylamine-modified polyacrylic acid.

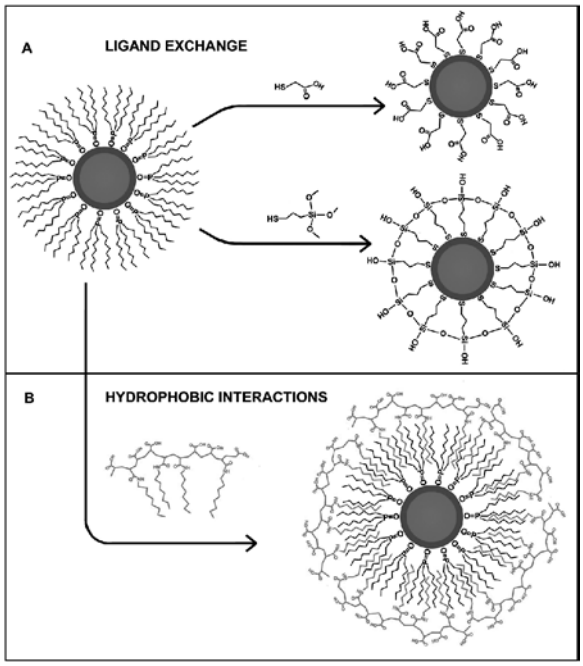

Figure 4. Diagram of two general strategies for phase transfer of TOPO-coated QD into aqueous solution. Ligands are drawn disproportionately large for detail, but the ligand–polymer coatings are usually only 1–2 nm in thickness. A: TOPO ligands may be exchanged for heterobifunctional ligands for dispersion in aqueous solution. This scheme can be used to generate hydrophilic QD with carboxylic acids or a shell of silica on the QD surfaces. B: The hydrophobic ligands may be retained on the QD surface and rendered water soluble through micelle-like interactions with an amphiphilic polymer-like octylamine-modified polyacrylic acid.

These polymers contain alkyl chains that are thought to interdigitate with hydrophobic TOPO ligands, leaving the hydrophilic carboxylic acid groups directed away from the QD surface. This later method is more effective than ligand exchange at maintaining the QD optical properties and storage stability in aqueous buffer, but it increases the overall size of QD probes.

Bioconjugation

Most solubilization methods result in a QD covered with carboxylic acid groups, and QD in aqueous buffers are regarded as negatively charged colloids. Many schemes used to prepare QD bioconjugates rely on covalent bond formation between carboxylic acids and biomolecules such as peptides, proteins and nucleic acids. Because the QD surface has a net negative charge, positively charged molecules could also be used for electrostatic conjugation, a technique that has been used to coat QD with cationic avidin proteins or recombinant maltose-binding proteins fused with positively charged peptides (36,37). Alternatively, biomolecules containing basic functional groups such as amines and thiols may interact directly with the surface of QD as ligands (25). If biomolecules do not contain groups for direct QD binding, they may be altered to add these functionalities; for example, nucleic acids and peptides can be modified with a thiol group for binding to QD (1,38). Surface modification has also become modular through high-affinity streptavidin–biotin binding (5). QD–streptavidin provides a convenient and indirect approach for linking to a broad range of biotinylated biomolecules.

APPLICATIONS IN MOLECULAR AND CELLULAR IMAGING

Fluorescence is a sensitive and routine method for monitoring biological events using fluorescent dyes and fluorescent proteins. During the past 5 years, QD have also been used as biological labels in a variety of bioassays, some of which would not have been possible with conventional fluorophores. *In vitro* bioanalytical assays were developed by using QD-tagged antibodies (39), fluorescence resonance energy transfer (FRET)–QD biosensors (7) as well as by using QD-encoded microbeads (8,40). In addition to solution-based assays, the spectroscopic advantages of QD should also benefit sensitive optical imaging in living cells and animal models (see Discussion below).

Imaging of fixed cells and tissues

Many methods are currently available to detect and characterize biomolecules and to monitor biological events *in vitro*. However, *in vitro* data can only yield a simplified model of what might actually occur within a complex living system. For example, current molecular profiling technologies such as biochips and mass spectrometry involve lysing cells or tissues into a homogeneous solution. This necessitates a loss of the cellular spatial information that describes where biological events occur within a cell or a heterogeneous cell population. This spatial information can be maintained through *in situ* staining of fixed cells and tissues. QD may be used to improve the sensitivity and multiplexing abilities of *in situ* staining due to their emission brightness and narrow fluorescence spectra. The feasibility of using QD for antigen detection in fixed cellular monolayers was first demonstrated by Bruchez and coworkers in 1998 (4). By labeling nuclear antigens with green silica-coated (CdSe)ZnS QD and F-actin filaments with red QD in fixed mouse fibroblasts, these two spatially distinct intracellular antigens were simultaneously detected. This article and others (2,5) have demonstrated that QD are brighter and dramatically more photostable than organic fluorophores when used for cellular labeling.

In recent research, many different cellular antigens in fixed cells and tissues have been labeled using QD, including specific genomic sequences (41,42) and antigens within paraffin-embedded tissue sections (43–45). Plasma membrane proteins, cytoplasmic proteins and nuclear proteins have all been labeled in fixed cells using QD, and it is apparent that they can function as both primary and secondary antibody stains (4,5,43,46,47). In addition, high-resolution actin filament imaging has been demonstrated using QD (5), and the fluorescence can be correlated directly to electron micrograph contrast due to the high electron density of QD (47). It has now become clear that QD can perform just as well and for many applications can perform better than organic fluorophores for fixed cell labeling.

Live cell imaging

In comparison with fixed cells and tissues, live cell labeling is a more difficult task because of care that must be taken to keep cells alive and because of the challenge of delivering probes across the plasma membrane for studying intracellular targets. The number of available probes for monitoring *in vivo* systems in real time is very limited. This may be one area of biology in which QD could make a significant impact because they have already shown promise as *in vitro* biosensors and live cell labels. The first study of using QD for live cell labeling was reported by Chan and Nie in 1998 (2). By

covalently conjugating mercaptoacetic acid–coated (CdSe)ZnS QD to the transferrin protein, QD were spontaneously endocytosed by cancer cells. This work demonstrated that QD retained their bright fluorescence *in vivo* and could be used as intracellular labels.

In vivo applications of QD have been slow to develop because of the technical difficulties associated with living cell studies. Nonetheless, it has been found that cellular surface antigens can be labeled using techniques like those used for fixed cells by means of antibody–antigen interactions or receptor–ligand interactions (Fig. 5) (5,6,48–50). For intracellular staining of cells, polyethylene glycol (PEG)–coated (CdSe)ZnS QD with green emission were microinjected into single cells of a *Xenopus* embryo (35). Microscopic fluorescence imaging allowed real-time monitoring of cell lineage and differentiation. Remarkably, most of the embryos exhibited normal development, and there was no evidence of toxicity, even with the injection of over 1 billion QD particles per cell (see the next section for a more detailed discussion on QD toxicity). Focusing on a simple multicellular organism, this report demonstrated the potential of QD in tagging and tracking living systems.

Recent work has highlighted the true advantages of QD for live cell imaging: the potential for real-time tracking of biomarkers due to minimal photobleaching and the sensitivity to image single molecules. Dahan *et al.* labeled the plasma membrane glycine receptor on neuronal cells using primary antibodies bound to QD with red emission (50). Real-time observation of the diffusion of single receptors was achieved for more than 20 min, with greater photostability and signal-to-noise ratios than the organic dye Cy3. In another report, Lidke *et al.* labeled erbB/HER receptors on the membranes of various cell types with QD conjugated to epidermal growth factor (EGF) (6). QD enabled the authors to watch EGF-receptor binding in real time and to observe the subsequent internalization of the receptor conjugate. By combining this labeling approach with fluorescent receptor fusion proteins, the data provided new insights into the mechanism of ligand–receptor interactions and also enabled the observation of a previously unidentified transport mechanism in filopodia.

For intracellular studies of living cells, four different mechanisms have been used to circumvent the plasma membrane barrier: microinjection, nonspecific uptake, protein- or peptide-specific uptake, and receptor–ligand uptake. Intracellular microinjection of probes is obviously useful for studying single cells, but it is difficult to obtain statistically relevant data because of the small number of cells that could be realistically injected. It has been found that the addition of water-soluble QD to the medium of cultured cells causes the nonspecific uptake of QD through an endocytotic mechanism (51). This is the basis for a cellular motility assay, in which the movement of cells over a substrate covered with silica-coated QD was measured in real time through the increase in fluorescence from the cells and the nonfluorescent ''dark'' path that they left behind (52). The third mechanism involves the conjugation of QD to either translocating proteins, such as transferrin, or cationic peptides, which cause cellular uptake through a mechanism that is still not clear (2,53). These first three mechanisms allow uptake from a wide variety of cell types. The fourth mechanism uses the induced uptake of ligand–QD conjugates through specific membrane receptor binding, like the aforementioned EGF ligand and erbB/HER receptor interaction (6,51). All four of these techniques have successfully delivered QD into cells, although it seems that the peptide mechanism may be the most efficient (Fig. 5). Targeting of these QD to specific intracellular locations for monitoring biological events will be a more difficult task, requiring both membrane permeability and biomolecular targeting.

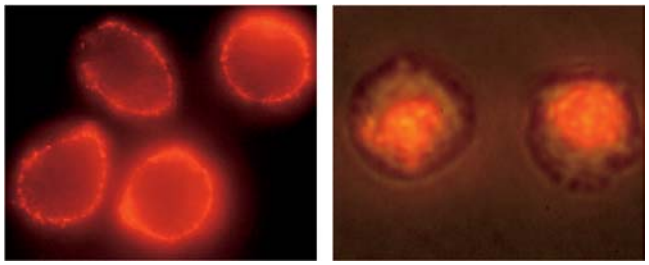

Figure 5. Fluorescent staining of living cancer cells using (CdSe)ZnS QD. Left: Cells were incubated with QD conjugated to an antibody against the uPAR cell surface receptor. Right: Cells were incubated with QD–TAT peptide conjugates. The cationic TAT peptide induced efficient internalization of the QD conjugates as well as QD localization in the cell nucleus.

In vivo animal imaging

Fluorescent proteins and small organic dyes have been used as fluorescent contrast agents for living animal imaging (54). The ideal fluorescent probe would contain a targeting domain with high affinity for a specific tissue after systemic delivery and a fluorescent domain that emits light on target binding. Preferably, the targeting domain would be modular so that any tissue could be imaged. As well, the probe must minimize nonspecific interactions, it must have long-term stability, and it should either be thoroughly excreted from the body or degraded with minimal toxicity. To benefit from the advantageous photophysical properties of QD as *in vivo* labels, a number of issues must be considered. First, the relatively large size and surface area of QD allow the attachment of multiple targeting probes to each label for enhanced binding specificity. However, this size (perhaps 4–20 nm diameter after bioconjugation) also has the disadvantage of being too large to penetrate through the vascular endothelium and too large to be excreted in the urine. The accessible targets for systemically administrated QD probes could be limited to those of vascular exposure, such as endothelial receptors. Also, nanoparticles are nonspecifically uptaken by phagocytic cells in the organs of the reticuloendothelial system (RES, most notably by the liver and spleen). This nonspecific targeting can be reduced by coating nanoparticles with hydrophilic polymers such as PEG to allow greater vascular circulation time, but nonspecific uptake cannot be eliminated completely (1,55,56).

The first report of systemic QD injection was by Akerman *et al.* in 2002, which demonstrated the targeting problems and nonspecific uptake associated with nanoparticle probes (1). In this *ex vivo* study, (CdSe)ZnS QD with either green or red emission were injected intravenously into mice. By attaching tissue-specific peptides to the QD, these nanoparticles were targeted to the lung vasculature, tumor vasculature or tumor lymphatic vessels. Fluorescence observation of mouse tissue sections showed uptake in the target tissue, but nonspecific uptake by the RES was also observed. This uptake is not a problem if the target organ is part of the RES, such as a lymph node. In 2003 Kim *et al.* fluorescently imaged murine and porcine sentinel lymph nodes after intradermal injection of NIR (CdTe)CdSe QD (29). Dendritic cells nonspecifically phagocytosed the injected QD, and then migrated to sentinel lymph nodes that could then be fluorescently detected even 1 cm under the skin surface. Nonspecific uptake is also not a

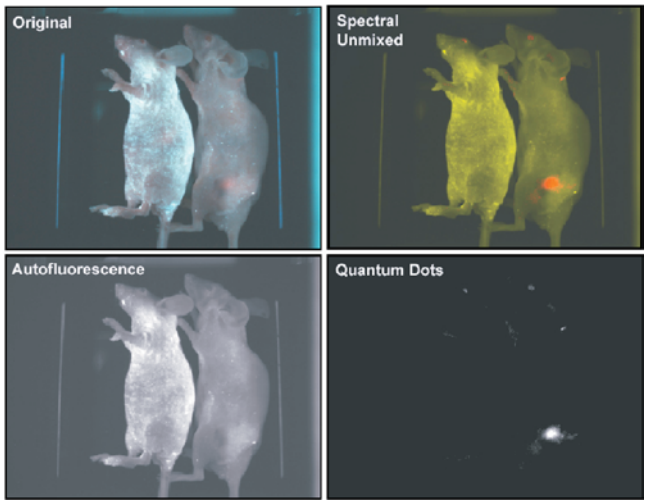

Figure 6. Spectral imaging of QD–prostate-specific membrane antigen (PSMA) Ab conjugates in live animals harbored with C4-2 tumor xenografts. Orange-red fluorescence signals indicate a prostate tumor growing in a live mouse (right). Control studies using a healthy mouse (no tumor) and the same amount of QD injection showed no localized fluorescence signals (left). (a) Original image, (b) unmixed autofluorescence image, (c) unmixed QD image, and (d) superimposed image. After *in vivo* imaging, histological and immunocytochemical examinations confirmed that the QD signals came from an underlying tumor. Note that QD in deep organs such as liver and spleen were not detected because of the limited penetration depth of visible light.

problem if imaging of the target tissue can be achieved before RES
?5 clearance becomes significant. To this end, QD were used as contrast agents for angiography after intravenous injection, first for imaging the coronary vasculature of rats (26) and later for imaging capillaries within skin and adipose tissue in mice (57).

In the previous example of mouse capillary imaging, the authors made use of two-photon excitation for *in vivo* QD imaging (57). Two-photon excitation allows greater tissue penetration due to excitation within the NIR spectral range, but the QD were fluorescent in the visible region. Near-UV and visible light have poor penetration through biological tissue more than 1 cm thick (27). This attenuation is due to scattering, absorption by water and absorption by biological chromophores such as hemoglobin. However, NIR light (>650 nm) is known to be attenuated less by biological tissue and, therefore, could serve as an optical window for fluorescent imaging. One of the main problems in NIR medical imaging has been the lack of fluorophores that are brightly emissive in the NIR, and can also be excited in the far red or NIR. Few organic fluorophores exist with both excitation and emission bands above 650 nm. Many types of QD have recently been developed with bright emission within this range (CdTe, CdSeTe, (CdTe)CdSe, PbS, PbSe QD) and, therefore, could propel the development of this field (17–19,58,59). Two of the aforementioned experiments made use of NIR QD, but so far there have been no experimental reports of the advantages of NIR *vs* visible QD, although a theoretical model has been described (26).

Before QD clinical applications become possible, the biocompatibility of these nanoparticles must be thoroughly investigated. For cell culture studies, a biocompatible particle must be nontoxic and must be inert and stable over the course of an assay. For studying organisms, a biocompatible particle must also be nonthrombogenic and nonimmunogenic. In short, this means making the particle as inert as possible, allowing its specific and intended function to be its only activity. PEG and other biologically inert polymers may be useful for rendering QD biocompatible. The long-term fate of QD injected into live animals must be studied if animal experiments are to become more than proof-of-principle projects. So far, nearly all the publications on the *in vivo* use of QD have reported normal organism development and no detectable toxicity (35,51,52,56,57,60). However, long-term stability has not been investigated, and it is unlikely that systemically administered QD will be completely cleared from the body before degradation. Recently, Derfus *et al.* used cultured liver cells to determine the cytotoxicity of (CdSe)ZnS QD with various surface coatings (61). The results suggested that surface coatings must be sufficiently stable to prevent oxidation of the QD surface, which results in the release of divalent cadmium, a known toxin and suspected carcinogen. For stability *in vivo*, the amphiphilic polymer approach for water solubility results in a robust hydrocarbon double layer and is a better choice than the ligand exchange method. If QD could be used clinically, much more cytotoxicity data is needed, especially in living animals, and QD surface-coating technologies must be well understood.

In vivo tumor targeting and imaging

The current gold standard to determine whether or not cells are cancerous is to test if they will grow as transplants in a nude mouse (lacking a thymus and functional immune system). This is also an excellent system for studying nanoparticle targeting and imaging *in vivo*. An implanted subdermal human tumor in a nude mouse is a controlled targeting system due to the presentation of highly specific xenograft antigens. As well, subdermal tumors only require a shallow penetration depth for imaging. Importantly, the vasculature of most cancer tissue is highly disordered, causing exposed interstitial tissue, so that tumor antigens are in direct contact with blood. Using such a model system, Gao *et al.* (62) recently succeeded in targeting and imaging human prostate tumors in mice after intravenous injection of PEG-coated QD that were conjugated to an antibody against the prostate-specific membrane antigen (Fig. 6). QD accumulation in the tumor was primarily due to antibody–antigen binding but was also aided by the enhanced permeability and retention (EPR) effect characteristic of many angiogenic tumors. The EPR effect is due to the inherent vascular permeability of the microenvironment of cancerous tissue, combined with a lack of lymphatic drainage, caused by the absence of a regional lymphatic network. Because of the EPR effect alone, it was found that nonconjugated PEG-QD accumulated in induced mouse tumors, demonstrating tumor contrast, but much less efficiently than actively targeted probes. This work was the first demonstration of targeted molecular imaging using QD in a living organism. Molecular imaging is the generation of image contrast due to the molecular differences in tissue, rather than the differences in tissue-induced radiation attenuation. Also in this work, multicolor imaging of QD-tagged cancer cells and QD-encoded microbeads was demonstrated. These results open new possibilities for ultrasensitive and simultaneous imaging of multiple biomarkers involved in cancer metastasis and invasion.

A major development is a new class of multifunctional QD probes with both tumor targeting and drug-delivery functions. As shown in Fig. 7, core-shell CdSe/ZnS QD are protected by both a coordinating ligand (TOPO) and an amphiphilic polymer coating. Because of strong hydrophobic interactions between TOPO and the polymer hydrocarbon, these two layers ''bond'' to each other and form a hydrophobic protection structure that is resistant against

hydrolysis and enzymatic degradation even under complex *in vivo* conditions. In contrast to simple polymers and amphiphilic lipids used in previous studies (5,35), Gao *et al*. (62) used a high molecular weight (100 kD) copolymer with an elaborate ABC triblock structure and a grafted 8-carbon (C-8) alkyl side chain. This triblock polymer consists of a polybutylacrylate segment (hydrophobic), a polyethylacrylate segment (hydrophobic), a polymethacrylic acid segment (hydrophilic) and a hydrophobic hydrocarbon side chain. A key finding is that this polymer can disperse and encapsulate single TOPO-capped QD by means of a spontaneous self-assembly process. As a result, the QD are protected to such a degree that their optical properties (*e.g*. absorption spectra, emission spectra and fluorescence quantum yields) did not change in a broad range of pH (1–14) and salt conditions (0.01–1 *M*) or after harsh treatment with 1.0 *M* hydrochloric acid (PEG-linked QD).

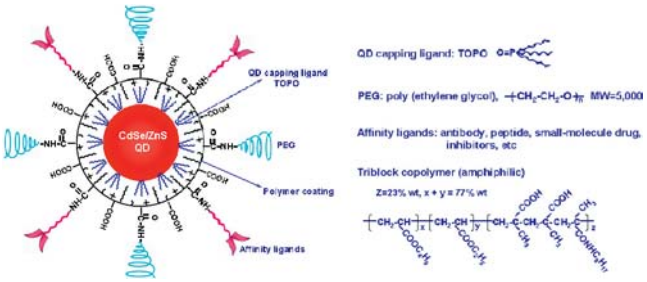

Figure 7. Structure of a multifunctional QD probe, showing the capping ligand TOPO, an encapsulating copolymer layer, tumor-targeting ligands (such as peptides, antibodies or small-molecule inhibitors) and polyethylene glycol (PEG).

FUTURE DIRECTIONS

Despite a recent burst in research and development activities, the use of QD for biological applications is much closer to its beginning than to its end. For example, few reports have made use of QD for NIR molecular imaging, although this should be one avenue that will make great advances because of the greater sensitivity and deeper tissue penetration that is possible in this spectral region. Another direction is to take advantage of the longer excited-state lifetimes (20–50 ns) of QD. Because most organic fluorophores and fluorescent proteins have fluorescent lifetimes on the order of 1–10 ns, the extended lifetimes of QD fluorescence could allow separation of QD fluorescence from background fluorescence for enhanced contrast.

A further promising area is the development of QD-based biosensors. Recently, Medintz *et al*. coated QD with maltose-binding protein for use as a maltose sugar sensor (7). By adding maltose conjugated to a nonemissive quenching dye to a solution of these QD, the dye quenched the fluorescence of the QD. Addition of a solution of maltose caused dissociation of the sugar–dye conjugate from the protein on the QD surface due to binding of native maltose. The maltose concentration was quantitatively determined from the QD fluorescence intensity. The mechanism of quenching in this case was due to FRET from the excited QD (the energy donor) to the dye (energy acceptor). The use of these sensing QD in living systems could provide information that is difficult or impossible to obtain without killing the cells or organisms. However, one of the barriers to making successful QD ''molecular beacons'' is the penetration of QD into cells and then targeting them to specific intracellular locations for sensing of specific events.

As research in nanoscience and nanotechnology continues to generate nanomaterials with novel properties, it should become possible to assemble miniscule particles or objects into complex, multifunctional devices, much in the same way that biological systems combine simple organic molecules to make complex structures (63). It has been suggested that the future of medicine lies within the nanometer regime and that nanometer-scale devices could be used to find a diseased tissue within a human and cure the disease while monitoring progress (64,65). Researchers have already begun building QD into larger biological structures for multifunctional use. One of the more practical endeavors has been the creation of multimodal imaging contrast agents, specifically by combining a QD for fluorescence imaging and a magnetic resonance imaging (MRI) contrast agent. Researchers have attached QD to Fe_2O_3 and FePt nanoparticles (66,67) and even to lanthanide chelates (X. Gao and S. Nie, unpublished). These composite particles could allow deep-tissue imaging using MRI for diagnosis and could be a fluorescent guide for a surgeon's scalpel during surgery. Another goal is the combination of a therapeutic drug with an imaging agent. This combination could be used to study the pharmacokinetics of drugs and also for monitoring of a therapy and diseased tissue during treatment, without the administration of a separate contrast agent. These combinations are only a few possible achievements for the future. Practical applications of these multifunctional nanodevices will not come without careful research but the multidisciplinary nature of nanotechnology may expedite these goals by combining the great minds of many different fields. The success seen so far with QD points toward the success of QD in biological systems and also predicts the success of other avenues of bionanotechnology.

Acknowledgements—This work was supported by a grant from the National Institutes of Health (R01 GM60562), the Georgia Cancer Coalition (Distinguished Cancer Scholar Award to S.N.) and the Coulter Translational Research Program at Georgia Tech and Emory University. A.M.S. acknowledges the Whitaker Foundation for generous fellowship support. X.G. was a Bioplex Fellow sponsored by the CrystalPlex Corporation (Pittsburgh, PA).

REFERENCES

1. Akerman, M. E., W. C. W. Chan, P. Laakkonen, S. N. Bhatia and E. Ruoslahti (2002) Nanocrystal targeting in vivo. *Proc. Natl. Acad. Sci. USA* **99**, 12617–12621.
2. Chan, W. C. W. and S. M. Nie (1998) Quantum dot bioconjugates for ultrasensitive nonisotopic detection. *Science* **281**, 2016–2018.
3. Parak, W. J., D. Gerion, D. Zanchet, A. S. Woerz, T. Pellegrino, C. Micheel, S. C. Williams, M. Seitz, R. E. Bruehl, Z. Bryant, C. Bustamante, C. R. Bertozzi and A. P. Alivisatos (2002) Conjugation of DNA to silanized colloidal semiconductor nanocrystalline quantum dots. *Chem. Mater*. **14**, 2113–2119.
4. Bruchez, M., M. Moronne, P. Gin, S. Weiss and A. P. Alivisatos (1998) Semiconductor nanocrystals as fluorescent biological labels. *Science* **281**, 2013–2016.
5. Wu, X. Y., H. J. Liu, J. Q. Liu, K. N. Haley, J. A. Treadway, J. P. Larson, N. F. Ge, F. Peale and M. P. Bruchez (2003) Immunofluorescent labeling of cancer marker Her2 and other cellular targets with semiconductor quantum dots. *Nat. Biotechnol*. **21**, 41–46.
6. Lidke, D. S., P. Nagy, R. Heintzmann, D. J. Arndt-Jovin, J. N. Post, H. E. Grecco, E. A. Jares-Erijman and T. M. Jovin (2004) Quantum dot ligands provide new insights into erbB/HER receptor-mediated signal transduction. *Nat. Biotechnol*. **22**, 198–203.
7. Medintz, I. L., A. R. Clapp, H. Mattoussi, E. R. Goldman, B. Fisher and J. M. Mauro (2003) Self-assembled nanoscale biosensors based on quantum dot FRET donors. *Nat. Mater*. **2**, 630–638.

8. Han, M. Y., X. H. Gao, J. Z. Su and S. Nie (2001) Quantum-dot-tagged microbeads for multiplexed optical coding of biomolecules. *Nat. Biotechnol.* **19**, 631–635.
9. Efros, Al. L. and A. L. Efros (1982) Interband absorption of light in a semiconductor sphere. *Sov. Phys. Semicond.* **16**, 772–775.
10. Ekimov, A. I. and A. A. Onushchenko (1982) Quantum size effect in the optical-spectra of semiconductor micro-crystals. *Sov. Phys. Semicond.* **16**, 775–778.
11. Jovin, T. M. (2003) Quantum dots finally come of age. *Nat. Biotechnol.* **21**, 32–33.
12. Alivisatos, A. P. (1996) Perspectives on the physical chemistry of semiconductor nanocrystals. *J. Phys. Chem.* **100**, 13226–13239.
13. Sutherland, A. J. (2002) Quantum dots as luminescent probes in biological systems. *Curr. Opin. Solid State Mater. Sci.* **6**, 365–370.
14. Peng, X. G. (2003) Mechanisms for the shape-control and shape-evolution of colloidal semiconductor nanocrystals. *Adv. Mater.* **15**, 459–463.
15. Qu, L. H. and X. G. Peng (2002) Control of photoluminescence properties of CdSe nanocrystals in growth. *J. Am. Chem. Soc.* **124**, 2049–2055.
16. Zhong, X. H., Y. Y. Feng, W. Knoll and M. Y. Han (2003) Alloyed $Zn_xCd_{1-x}S$ nanocrystals with highly narrow luminescence spectral width. *J. Am. Chem. Soc.* **125**, 13559–13563.
17. Bailey, R. E. and S. M. Nie (2003) Alloyed semiconductor quantum dots: tuning the optical properties without changing the particle size. *J. Am. Chem. Soc.* **125**, 7100–7106.
18. Kim, S., B. Fisher, H. J. Eisler and M. Bawendi (2003) Type-II quantum dots: CdTe/CdSe(core/shell) and CdSe/ZnTe(core/shell) heterostructures. *J. Am. Chem. Soc.* **125**, 11466–11467.
19. Wehrenberg, B. L., C. J. Wang and P. Guyot-Sionnest (2002) Interband and intraband optical studies of PbSe colloidal quantum dots. *J. Phys. Chem. B* **106**, 10634–10640.
20. Alivisatos, A. P. (1996) Semiconductor clusters, nanocrystals, and quantum dots. *Science* **271**, 933–937.
21. Murphy, C. J. and J. L. Coffer (2002) Quantum dots: a primer. *Appl. Spectrosc.* **56**, 16A–27A.
22. Sapra, S. and D. D. Sarma (2004) Evolution of the electronic structure with size in II-VI semiconductor nanocrystals. *Phys. Rev. B* **69**, 125304.
23. Yoffe, A. D. (2001) Semiconductor quantum dots and related systems: electronic, optical, luminescence and related properties of low dimensional systems. *Adv. Phys.* **50**, 1–208.
24. Brus, L. E. (1984) Electron electron and electron-hole interactions in small semiconductor crystallites—the size dependence of the lowest excited electronic state. *J. Chem. Phys.* **80**, 4403–4409.
25. Gao, X. H., W. C. W. Chan and S. M. Nie (2002) Quantum-dot nanocrystals for ultrasensitive biological labeling and multicolor optical encoding. *J. Biomed. Opt.* **7**, 532–537.
26. Lim, Y. T., S. Kim, A. Nakayama, N. E. Stott, M. G. Bawendi and J. V. Frangioni (2003) Selection of quantum dot wavelengths for biomedical assays and imaging. *Mol. Imaging* **2**, 50–64.
27. Weissleder, R. (2001) A clearer vision for in vivo imaging. *Nat. Biotechnol.* **19**, 316–317.
28. Frangioni, J. V. (2003) In vivo near-infrared fluorescence imaging. *Curr. Opin. Chem. Biol.* **7**, 626–634.
29. Kim, S., Y. T. Lim, E. G. Soltesz, A. M. De Grand, J. Lee, A. Nakayama, J. A. Parker, T. Mihaljevic, R. G. Laurence, D. M. Dor, L. H. Cohn, M. G. Bawendi and J. V. Frangioni (2004) Near-infrared fluorescent type II quantum dots for sentinel lymph node mapping. *Nat. Biotechnol.* **22**, 93–97.
30. Talapin, D. V., A. L. Rogach, A. Kornowski, M. Haase and H. Weller (2001) Highly luminescent monodisperse CdSe and CdSe/ZnS nanocrystals synthesized in a hexadecylamine-trioctylphosphine oxide-trioctylphospine mixture. *Nano Lett.* **1**, 207–211.
31. Hines, M. A. and P. Guyot-Sionnest (1996) Synthesis and characterization of strongly luminescing ZnS-capped CdSe nanocrystals. *J. Phys. Chem.* **100**, 468–471.
32. Nirmal, M. and L. Brus (1999) Luminescence photophysics in semiconductor nanocrystals. *Acc. Chem. Res.* **32**, 407–414.
33. Peng, X. G., M. C. Schlamp, A. V. Kadavanich and A. P. Alivisatos (1997) Epitaxial growth of highly luminescent CdSe/CdS core/shell nanocrystals with photostability and electronic accessibility. *J. Am. Chem. Soc.* **119**, 7019–7029.
34. Reiss, P., J. Bleuse and A. Pron (2002) Highly luminescent CdSe/ZnSe core/shell nanocrystals of low size dispersion. *Nano Lett.* **2**, 781–784.
35. Dubertret, B., P. Skourides, D. J. Norris, V. Noireaux, A. H. Brivanlou and A. Libchaber (2002) In vivo imaging of quantum dots encapsulated in phospholipid micelles. *Science* **298**, 1759–1762.
36. Mattoussi, H., J. M. Mauro, E. R. Goldman, G. P. Anderson, V. C. Sundar, F. V. Mikulec and M. G. Bawendi (2000) Self-assembly of CdSe-ZnS quantum dot bioconjugates using an engineered recombinant protein. *J. Am. Chem. Soc.* **122**, 12142–12150.
37. Goldman, E. R., E. D. Balighian, H. Mattoussi, M. K. Kuno, J. M. Mauro, P. T. Tran and G. P. Anderson (2002) Avidin: a natural bridge for quantum dot-antibody conjugates. *J. Am. Chem. Soc.* **124**, 6378–6382.
38. Mitchell, G. P., C. A. Mirkin and R. L. Letsinger (1999) Programmed assembly of DNA functionalized quantum dots. *J. Am. Chem. Soc.* **121**, 8122–8123.
39. Goldman, E. R., A. R. Clapp, G. P. Anderson, H. T. Uyeda, J. M. Mauro, I. L. Medintz and H. Mattoussi (2004) Multiplexed toxin analysis using four colors of quantum dot fluororeagents. *Anal. Chem.* **76**, 684–688.
40. Xu, H. X., M. Y. Sha, E. Y. Wong, J. Uphoff, Y. H. Xu, J. A. Treadway, A. Truong, E. O'Brien, S. Asquith, M. Stubbins, N. K. Spurr, E. H. Lai and W. Mahoney (2003) Multiplexed SNP genotyping using the Qbead (TM) system: a quantum dot-encoded microsphere-based assay. *Nucleic Acids Res.* **31**, e43.
41. Pathak, S., S. K. Choi, N. Arnheim and M. E. Thompson (2001) Hydroxylated quantum dots as luminescent probes for in situ hybridization. *J. Am. Chem. Soc.* **123**, 4103–4104.
42. Xiao, Y. and P. E. Barker (2004) Semiconductor nanocrystal probes for human metaphase chromosomes. *Nucleic Acids Res.* **32**, e28.
43. Sukhanova, A., M. Devy, L. Venteo, H. Kaplan, M. Artemyev, V. Oleinikov, D. Klinov, M. Pluot, J. H. M. Cohen and I. Nabiev (2004) Biocompatible fluorescent nanocrystals for immunolabeling of membrane proteins and cells. *Anal. Biochem.* **324**, 60–67.
44. Ness, J. M., R. S. Akhtar, C. B. Latham and K. A. Roth (2003) Combined tyramide signal amplification and quantum dots for sensitive and photostable immunofluorescence detection. *J. Histochem. Cytochem.* **51**, 981–987.
45. Sukhanova, A., L. Venteo, J. Devy, M. Artemyev, V. Oleinikov, M. Pluot and I. Nabiev (2002) Highly stable fluorescent nanocrystals as a novel class of labels for immunohistochemical analysis of paraffin-embedded tissue sections. *Lab. Invest.* **82**, 1259–1261.
46. Alexson, D., Y. Li, D. Ramadurai, P. Shi, L. George, L. George, M. Uddin, P. Thomas, S. Rufo, M. Dutta and M. A. Stroscio (2004) Binding of semiconductor quantum dots to cellular integrins. *IEEE T. Nanotechnol.* **3**, 86–92.
47. Nisman, R., G. Dellaire, Y. Ren, R. Li and D. P. Bazett-Jones (2004) Application of quantum dots as probes for correlative fluorescence, conventional, and energy-filtered transmission electron microscopy. *J. Histochem. Cytochem.* **52**, 13–18.
48. Minet, O., C. Dressler and J. Beuthan (2004) Heat stress induced redistribution of fluorescent quantum dots in breast tumor cells. *J. Fluoresc.* **14**, 241–247.
49. Rosenthal, S. J., A. Tomlinson, E. M. Adkins, S. Schroeter, S. Adams, L. Swafford, J. McBride, Y. Q. Wang, L. J. DeFelice and R. D. Blakely (2002) Targeting cell surface receptors with ligand-conjugated nanocrystals. *J. Am. Chem. Soc.* **124**, 4586–4594.
50. Dahan, M., S. Levi, C. Luccardini, P. Rostaing, B. Riveau and A. Triller (2003) Diffusion dynamics of glycine receptors revealed by single-quantum dot tracking. *Science* **302**, 442–445.
51. Jaiswal, J. K., H. Mattoussi, J. M. Mauro and S. M. Simon (2003) Long-term multiple color imaging of live cells using quantum dot bioconjugates. *Nat. Biotechnol.* **21**, 47–51.
52. Parak, W. J., R. Boudreau, M. Le Gros, D. Gerion, D. Zanchet, C. M. Micheel, S. C. Williams, A. P. Alivisatos and C. Larabell (2002) Cell motility and metastatic potential studies based on quantum dot imaging of phagokinetic tracks. *Adv. Mater.* **14**, 882–885.
53. Pinaud, F., D. King, H. P. Moore and S. Weiss (2004) Bioactivation and cell targeting of semiconductor CdSe/ZnS nanocrystals with phytochelatin-related peptides. *J. Am. Chem. Soc.* **126**, 6115–6123.
54. Bremer, C. and R. Weissleder (2001) Molecular imaging—in vivo imaging of gene expression: MR and optical technologies. *Acad. Radiol.* **8**, 15–23.
55. Brigger, I., C. Dubernet and P. Couvreur (2002) Nanoparticles in cancer therapy and diagnosis. *Adv. Drug Deliv. Rev.* **54**, 631–651.

56. Ballou, B., B. C. Lagerholm, L. A. Ernst, M. P. Bruchez and A. S. Waggoner (2004) Noninvasive imaging of quantum dots in mice. *Bioconjugate Chem.* **15**, 79–86.
57. Larson, D. R., W. R. Zipfel, R. M. Williams, S. W. Clark, M. P. Bruchez, F. W. Wise and W. W. Webb (2003) Water-soluble quantum dots for multiphoton fluorescence imaging in vivo. *Science* **300**, 1434–1436.
58. Hines, M. A. and G. D. Scholes (2003) Colloidal PbS nanocrystals with size-tunable near-infrared emission: observation of post-synthesis self-narrowing of the particle size distribution. *Adv. Mater.* **15**, 1844–1849.
59. Yu, W. W., Y. A. Wang and X. G. Peng (2003) Formation and stability of size-, shape-, and structure-controlled CdTe nanocrystals: ligand effects on monomers and nanocrystals. *Chem. Mater.* **15**, 4300–4308.
60. Hoshino, A., K. Hanaki, K. Suzuki and K. Yamamoto (2004) Applications of T-lymphoma labeled with fluorescent quantum dots to cell tracing markers in mouse body. *Biochem. Biophys. Res. Commun.* **314**, 46–53.
61. Derfus, A. M., W. C. W. Chan and S. N. Bhatia (2004) Probing the cytotoxicity of semiconductor quantum dots. *Nano Lett.* **4**, 11–18.
62. Gao, X. H., Y. Cui, R. M. Levenson, L. W. K. Chung and S. Nie (2004) *Nat. Biotechnol.* In press. **?4**
63. Niemeyer, C. M. (2003) Functional hybrid devices of proteins and inorganic nanoparticles. *Angew. Chem. Int. Edit.* **42**, 5796–5800.
64. Levy, L., Y. Sahoo, K. S. Kim, E. J. Bergey and P. N. Prasad (2002) Nanochemistry: synthesis and characterization of multifunctional nanoclinics for biological applications. *Chem. Mater.* **14**, 3715–3721.
65. Alivisatos, A. P. (2001) Less is more in medicine. *Sci. Am.* **285**, 66–73.
66. Wang, D. S., J. B. He, N. Rosenzweig and Z. Rosenzweig (2004) Superparamagnetic Fe_2O_3 beads-CdSe/ZnS quantum dots core-shell nanocomposite particles for cell separation. *Nano Lett.* **4**, 409–413.
67. Gu, H. W., R. K. Zheng, X. X. Zhang and B. Xu (2004) Facile one-pot synthesis of bifunctional heterodimers of nanoparticles: a conjugate of quantum dot and magnetic nanoparticles. *J. Am. Chem. Soc.* **126**, 5664–5665.